Electronified Open Circuit Drive Concept for Compact Loaders

Xiaofan Guo, Shaoyang Qu, Rafael Cardoso, Enrique Busquets

Xiaofan Guo, Bosch Rexroth Corp., Xiaofan.Guo@boschrexroth-us.com

Shaoyang Qu, Bosch Rexroth Corp., Shaoyang.Qu@boschrexroth-us.com

Rafael Cardoso, Bosch Rexroth Corp., Rafael.Cardoso@boschrexroth-us.com

Enrique Busquets, Bosch Rexroth Corp., Enrique.Busquets@boschrexroth-us.com

Abstract.

The drive function of compact loader applications typically relies on closed-circuit hydrostatic transmission as a mature solution. This study adapts an innovative concept termed Electronified Open Circuit Drive (eOC-D), incorporating three open-circuit units, one pump to drive two motors, offering stepless speed control for the hydrostatic transmission. This innovative eOC-D concept is derived from the electronified open-circuit (eOC) unit by Rexroth. With four-quadrant capabilities in terms of displacement and speed, the eOC unit can smoothly transition from negative to position displacement, functioning as both a pump and a motor. Consequently, the eOC-D concept enhances drive performance through advanced electronic control of pressure, flow, torque, and power. In addition, the eOC-D approach leads to a significant reduction in component costs when compared to the closed-circuit architecture. To prove the concept, a simulation model is developed in the Simulink environment utilizing the lumped-parameter method with a 67kW power-rated compact loader as reference machine. Through simulations, the eOC-D system is sized considering an optimal combination of pump, motor, and gearbox. The performance of energy efficiency and dynamic response is evaluated from simulation. With baseline measurements as inputs, the eOC-D system demonstrates higher efficiencies and faster response compared to the baseline The efficiency improvement ranges from 5% to 10%, while the response time sees a reduction of over 50%.

Keywords. Open circuit drive, Hydrostatic transmission, Secondary control, Stepless speed control.

1. INTRODUCTION

1.1. State of the art

Hydrostatic transmission (HT) is a well-known solution for the transmission system of off-road vehicles [1] including construction machine, agriculture vehicle, forestry equipment and more. The advantages of simple design, robustness, and cost effectiveness is the key for its success. HT design normally has a variable displacement pump (P) close loop coupled (Line A and Line B) with a fixed or two-position motor (M) as depicted in Figure 1. A charge circuit (CP and PRC) is needed to provide control pressure for the pump and motor, as well as replenish the close loop hydraulic circuit according to unit volumetric loss and flushing flow (FV). Two pairs of pressure relief (PRA and PRB) and check valves (CVA and CVB) are installed to protect the system from over-pressurize or cavitation.

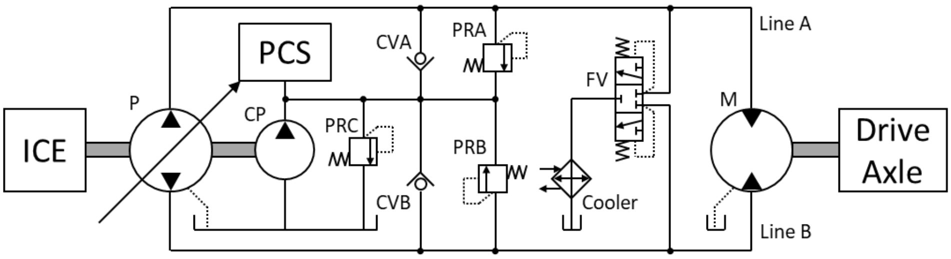

Figure 1. Hydrostatic Transmission Design

There are some significant alternatives on the design of the HT other than what is shown in Figure 1. Some great studies are [2] [3] [4] [5], and the difference are focus on charge circuit, different number of motors acting as multiple stage motor, configuration variation of series or parallel motor, and flushing, which does not change the fundamental design of the HT.

HT is a simple hydraulic circuit, but it still requires many components. For the reference machine in this study, compact track loader, there are two set of HT system. In total there are two primary units, two secondary units, four high pressure relief valves, four check valves, two flushing valves for cooling and recirculation, and two charge circuits. All these components cost money and take space. In addition to components, the charge circuits are always consuming power and creates parasitic loss [6].

To reduce the complexity and cost of the state-of-the-art transmission system with better system flexibility, the open-circuit drive concept has emerged as a great candidate motivated by increasing interest from the market thanks to the enormous improvement and cost reduction of the control unit and sensor technology. The innovative electronified open-circuit pump (eOC-P) technology from Rexroth makes the concept possible, termed Electronified Open Circuit Drive (eOC-D) in this study. Figure 2 illustrates the eOC-P technology, which uses the sensor feedback to accomplish for its capability in fast and accurate pressure and displacement control, as well as various working modes [7]. The most recent related work is done by Tetik and Brand [7]. They proposed an eOC-D system and control strategy for a small-sized tractor and showed great result on system performance.

The eOC units can serve as pump and motor with 4-quadrant operation in terms of speed and displacement. Consequently, the drive function can be achieved by one eOC pump and two eOC motors. In contrast to the traditional hydrostatic transmission, the eOC-D approach leads to a significant reduction in component costs. Only one drive pump is required instead of two, a single relief valve serves the open circuit instead of four, and the necessity for a charge pump is eliminated. Furthermore, the design enables the potential for energy regeneration during braking conditions, making use of the four-quadrant capability inherent in the EOC units.

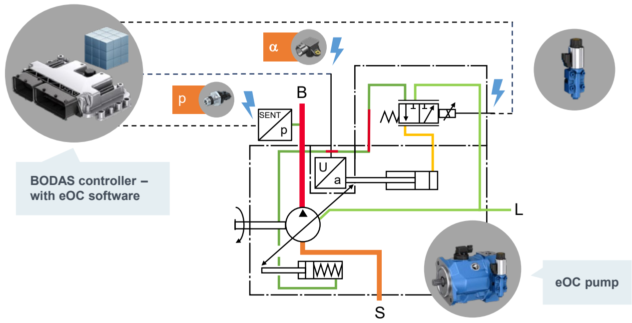

Figure 2. The electronified open-circuit pump (eOC-P) technology

For HT system control, the sequential control strategy is the most common way to manipulate the output speed of the drive. Machine starts at zero pump displacement at stand still. Then, increase the pump displacement to accelerate till hit maximum pump displacement, and the vehicle reaches maximum speed for fixed displacement motor. For two position motor, shift down to the lower motor displacement will reduce torque output but reach higher maximum vehicle speed. The eOC-D concept follows a similar control principle. However, compared to the conventional HT system, the eOC-D concept is capable of secondary control, offering stepless speed control for the transmission. Through advanced electronic control of pressure, flow, torque and power, an enhanced controllability can be achieved for the context of dynamic behavior and energy efficiency.

1.2. Goal and Structure

In contrast to the state-of-the-art architecture, the proposed eOC-D concept presents the following advantages:

- Reduced number of components and corresponding cost savings.
- Enhanced drive performance such as the faster response and better efficiencies.

The goal of this study is to define and optimize an all-in-one hydraulic system for mini-compact track loader (CTL) that powers transmission, implements, and aux systems using one supply pump equipped with secondary control strategy that could achieve same level of performance and efficiency.

This study is structured as follows: Chapter 2 showcases the proposed new one pump solution with hydraulic circuit design and sizing. Chapter 3 describes the control strategy for the secondary controlled transmission system and the implement systems. Chapter 4 lays out the simulation methodology adapted in this study and the simulation results, which reveal the drive cycle and compare both steady state driving system efficiency and dynamic driving performance. Finally, Chapter 5 concludes the study.

2. PROPOSED ARCHITECTURE

2.1. Reference Machine

The reference machine for this study is CAT 259D3 compact track loader as presented in Figure 3. It is a mid-power range CTL that equipped with duel hydrostatic transmission and closed centre load sensing implement hydraulic system.

Figure 3. Reference Machine CAT 259D3

The components and their details are listed in the Table 1.

Table 1. Component Information for Reference Machine.

Parameters	Description	Detail
Engine	Cat C3.3B DIT (turbo)	2500rpm rated speed
Hydrostatic Pump (V_P)	Axial piston variable displacement pump	45cc close-loop pump directly connect to engine
Hydrostatic Motor (V_M)	Axial piston two position motor	45cc close-loop motor connect to track drive through planetary gear set
Drive Gear (i_D)	Planetary Gear Set	18.47 gear ratio
Maximum Pressure Drop (Δp_{max})	-	350bar
Required Speed (v_{max})	Maximum speed for high and low gear	9.5km/h and 13.7km/h
Sprocket Radius (r_D)	-	0.2m

2.2. *Proposed Architecture*

This section will introduce the proposed architecture on hydraulic circuit and the component sizing.

2.2.1. *Hydraulic Circuit*

Figure 4 depicts the proposed eOC-D hydraulic circuit, highlighting the traction function. The target is to use one eOC unit for all functions, but this study mainly investigates the control of the drive track. Two eoc units are employed for the left and right track, and either of them can switch from positive to negative displacement for forwards or backwards movement.

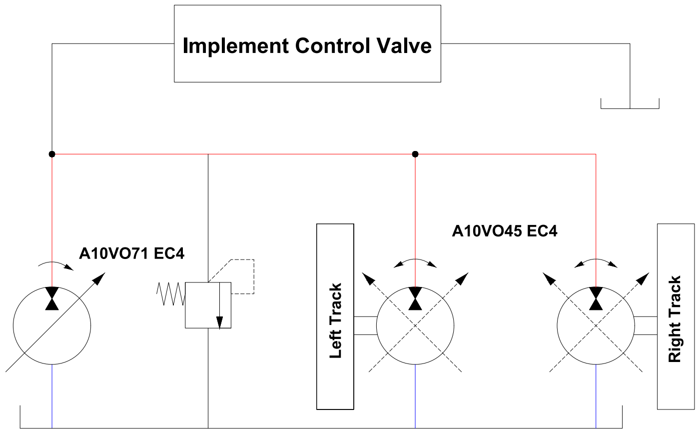

Figure 4. Proposed hydraulic schematic with simplified implement functions.

2.2.2. System Sizing

To ensure the proposed system achieve at least the same if not better performance, all the components need to be sized correctly. The benchmark is the vehicle travel speed and maximum traction force output.

The sizing starts from the maximum force output which determines the motor size and gear ratio. The pool for eOC unit, pump and motor, is 28cc, 45cc, 63cc, 71cc, and 88cc. The corresponding parameters of these units are in table below. The maximum pump flow q_P is calculated using equation (1), where the volumetric efficiency η_{VM} is assumed at 90%.

$$q_P = V_P \omega_P \eta_{VM} \tag{1}$$

Table 2. eOC Unit Pool and Key Parameters.

$V_{P/M}\ \left[\frac{cc}{rev}\right]$	28cc (P/M)	45cc (P/M)	63cc (M only)	71cc (P Only)	88cc (P Only)
$V_{M_{min}}\ \left[\frac{cc}{rev}\right]$	8cc	12cc	16cc	-	-
$Max.\Delta p\ [bar]$	315	315	315	315	280
$Max.\omega_{P/M}\ [rpm]$	3000/4700	2600/4000	-/3300	2200/-	2100/-
$Max.q_P\ [lpm]$	75.6	105	-	141	166

Defining the gear ratio as i_D, the maximum traction force output is calculated from equation (2).

$$F_{tr} = T_M \frac{i_D \eta_i}{r_D} = \frac{V_M \Delta p_{max}}{2\pi} \eta_{HM} \frac{i_D \eta_i}{r_D} = \frac{V_M \Delta p_{max} i_D}{2\pi r_D} \eta_{HM} \eta_i \tag{2}$$

F_{tr} is the traction force generated by one hydrostatic transmission powered track, T_M is the motor output torque, η_i is the planetary gear set efficiency (assume to be 97%), η_{HM} is the hydromechanical efficiency of the motor (assume to be 90%). The maximum force output is around 20kN for one track from the reference machine data. From equation (2), the gear ratio (i_D) to fulfil the traction force with given motor size could be calculated, as indicated in Table 3. Taking the maximum vehicle speed into consideration, the rotational speed with each motor could be calculated using equation (3), with the calculated gear ratio (i_D) from the traction force calculation. The results are summarized in Table 3.

$$\omega_{M_{max}} = \frac{v_{max}}{r_D} i_D \quad (3)$$

Table 3. Ideal Gear Ratio and Corresponding Maximum Motor Speed.

$V_M \left[\frac{cc}{rev}\right]$	28cc	45cc	63cc
i_D [−]	32.98	20.52	14.66
$\omega_{M_{max}}$ [rpm]	5993	3729	2664

From the result and compared to Table 2, 28cc motor is out due to over speed at maximum vehicle velocity. 71cc and 88cc cannot operate as motor. From a quick search on possible size of the gearbox, a ratio of 20.88 is available. As a result, **45cc motor** and **20.88 gear ratio** is selected. To meet the maximal torque requirement, the pump needs 315bar as the nominal pressure. As the 88cc unit cannot meet the pressure requests yet, **71cc pump** is selected for the proposed eOC-D system. Figure 5 illustrates the FADI plots, where the black indicates the baseline machine, and the red represents the speed – traction of the selected eOC-D components. From point 1 to 2, the motor stays at the maximal displacement, while the pump displacement increases for higher vehicle velocity. At point 2 the pump reaches the maximum displacement. From point 2 to point 3, the motors displacement decreases until meeting the peak velocity of the vehicle (13.7km/h) on paper. Regarding the black curves, point 4 to 5 depicts the first gear, and point 6 to 7 represents the second gear option with maximal potential speed. It is possible to extend point 3 to cover point 7 as the eOC motor displacement can be decreased further, but here it follows the specifications on paper.

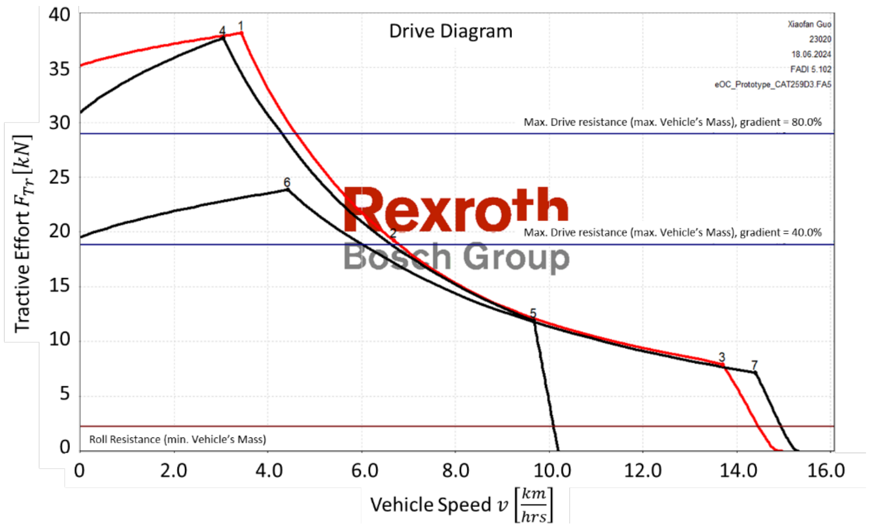

Figure 5. Sizing plots in FADI for the proposed eOC-D system.

The flow needed for the implement function is also taken into consideration. In this scenario, the minimum motor displacement of the motor (as shown in Table 2) is used for the calculation assuming the vehicle can run at maximum speed at this minimum motor displacement. Then the needed pump flow q_P could be calculated using equation (4). q_M is the required motor flow, q_{imp} is the required implement flow which is planned to be added in to the eOC system as next step. The selected 71cc pump can supply about 148lpm flow with a speed 2200rpm and 95% volumetric efficiency. For the baseline vehicle, the maximal speed of the first gear is 9.67km/h, which indicates a motor speed of about 2680rpm from equation (3). If the 45cc motor is commanded to the minimal displacement 12cc, both motors would need about 70lpm flow for the required speed, and about 78lpm flow is available for the implement functions. It fulfils the standard flow requests 76lpm for the reference machine implement functions.

$$q_P = \sum q_M + q_{imp} = \frac{2V_M \beta_M \omega_M}{\eta_{VM}} + q_{imp} \tag{4}$$

3. Controller Design

This section introduces the control strategy adapted for the proposed eOC drive system in detail. Tetik et al. [7] did a great job on laying out the control strategy for a small-sized tractor which has one drive motor with torque-based drive controller. For the chosen application of CTL in this study, the controller need modification as it contains two drive motors and follows close-loop speed-based drive controller. The overall controller of the eOC drive system contains pump/motor displacement control, vehicle speed/steering control, supply pressure selection and control, anti-stall control for both the drive and engine, and the following sections explains each control design in detail.

3.1. Pump/Motor Displacement Controller

The base level control of the proposed architecture is the eOC unit displacement controller. As presented in Figure 6, it uses a PID controller with scheduled gains with respect to pump operation condition: displacement β_{act}, pump outlet pressure p_P, and rotational speed ω_{act}. It takes the commanded displacement β_{cmd} as input and the measured displacement as feedback to form a close-loop control. Control valve current i_{ctrl} to the eOC unit is the output of the controller that directly send to the control valve which regulates the pressure in the control piston chamber to move the swashplate.

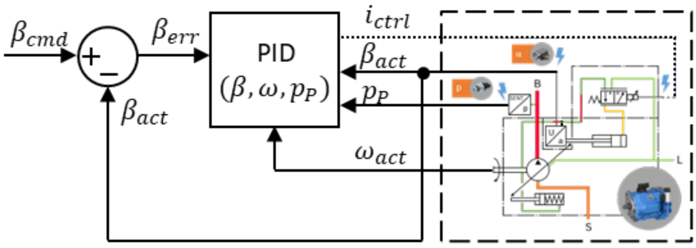

Figure 6. Pump/Motor Displacement Controller.

3.2. *Drive/Steering Controller*

This is the core controller for the CTL prototype. First, user will input desired drive/steering command using joystick. Then, these commands need to be converted to track desired speed for both left and right track. This is done through equation (5) and (6). cmd_{dr} and cmd_{st} indicating the user drive and steering command (from -100% to 100%), $v_{dr_{max}}$ and $\omega_{st_{max}}$ are the maximum drive speed (m/s) and steering rate (rad/s). $v_{cmd_{trL/R}}$ is the corresponding track speed (m/s) command from the drive and steering command. l_{tr} is the distance (m) between the centre line of left and right tracks.

$$v_{cmd_{trL}} = cmd_{dr} v_{dr_{max}} + cmd_{st} \omega_{st_{max}} l_{tr} \tag{5}$$

$$v_{cmd_{trR}} = cmd_{dr} v_{dr_{max}} - cmd_{st} \omega_{st_{max}} l_{tr} \tag{6}$$

If the drive and steering command cannot be met at the same time due to maximum speed limitation of the machine, the steering function holds priority. One example of this condition is the driver commands full speed forward and wants to steer to one side. Because the drive speed is the average of both track and neither track should exceed maximum speed, steering at full speed command will need to slow down one track to keep the speed difference between two tracks as demand to fulfil the steering command. In this situation, the drive speed will be lower than command, but the steering will execute successfully.

With the speed command for left and right track, Figure 7 illustrates the controller design. This controller is on the outer loop of the pump/motor displacement controller in green, so it is a cascade control structure. The command speed $v_{cmd_{tr}}$ and measured speed $v_{act_{tr}}$ are feed into the PID controller. The output of the controller is defined to be the command torque $T_{cmd_{tr}}$ for the motor to accelerate or decelerate the vehicle for speed tracking. Then, this torque is open-loop feedforward controlled to determine the corresponding motor displacement $\beta_{cmd_{tr}}$. This command displacement is sent to the pump/motor displacement controller introduced in section 3.1. With the actual displacement $\beta_{act_{tr}}$ at the motor and the supply pressure p_P, the actual torque $T_{act_{tr}}$ is sent to the track to manipulate machine speed.

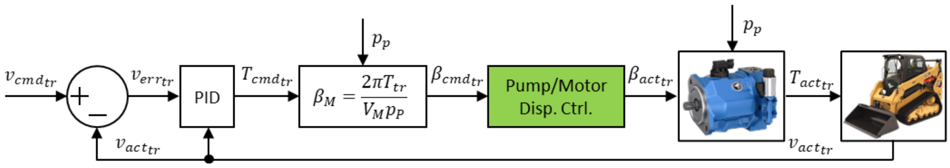

Figure 7. CTL Track Speed Controller.

In this controller, it is important for the PID controller output to be desired torque and go through one more calculation to get motor displacement command instead of directly commanding the motor displacement. The reason is twofold. On the one hand, without this step the system is oversimplified and missed the important coupling effect due to the supply pressure and will become very hard to reach an acceptable speed tracking performance. On the other hand, the desired torque could be used to determine the appropriate supply pressure for the drive system to achieve the best performance and system efficiency.

3.3. System Supply Pressure Controller

The supply pressure of the system determines how drive and implement system behaves and thus the overall performance and efficiency. The implement system required pressure $p_{cmd_{imp}}$ is straight forward, which is the highest load pressure $p_{imp_{max}}$ plus a certain margin p_{mar} to ensure the control valve has enough pressure drop to work properly as shown in equation (7).

$$p_{cmd_{imp}} = p_{imp_{max}} + p_{mar} \tag{7}$$

For the drive system, it is not that simple. The hydraulic motor can output same torque with infinite number of combinations of displacement and supply pressure. This provides the control freedom to choose the optimal pressure that provide maximum overall system efficiency. The hydraulic units are most efficient at high displacement and middle-to-high pressure [1]. As a result, the principle adapt in this study is to keep the motor displacement as high as possible. To find the corresponding pressure with maximum motor displacement, the desired torque from the track speed controller in section 3.2 is used. By assuming the motor at maximum displacement with 90% hydromechanical efficiency η_{HM}, equation (8) is used to calculate the desired supply pressure for the drive system. This calculation needs to be done for both left and right track motor.

$$p_{cmd_{dr}} = \max\left(\frac{2\pi T_{cmd_{tr_L}}}{V_M \eta_{HM}}, \frac{2\pi T_{cmd_{tr_R}}}{V_M \eta_{HM}}\right) \tag{8}$$

With both required pressure for implement and drive system, the final supply pressure is chosen using equation (9).

$$p_{cmd_P} = \max\left(p_{cmd_{imp}}, p_{cmd_{dr}}\right) \tag{9}$$

The system supply pressure control is critical for the proposed eOC drive system speed tracking performance. An accurate pressure controller can benefit the system on both efficiency and dynamic performance. Figure 8 depicts the pressure controller structure.

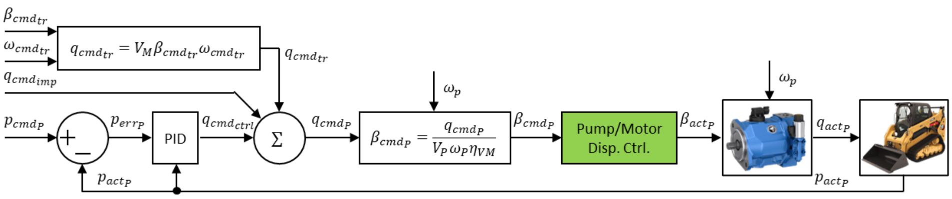

Figure 8. System Supply Pressure Controller.

It is a feedback-feedforward control structure based on flow logic. The total required flow q_{cmd_P} for both the drive $q_{cmd_{tr}}$ and implement $q_{cmd_{imp}}$ system is estimated from the command motor speed $\omega_{cmd_{tr}}$ with instantaneous command motor displacement $\beta_{cmd_{tr}}$ for both tracks and implement flow requirement $q_{cmd_{imp}}$. And a close-loop pressure PID controller is implemented to adjust the flow required $q_{cmd_{ctrl}}$ from the pump to match the command pressure. Then, the command pump displacement β_{cmd_P} is sent to the pump/motor displacement controller. Finally, the pump, with the actual displacement β_{act_P}, output flow q_{act_P} to the proposed eOC system.

3.4. *Engine Anti-Stall Controller*

Another advantage of the proposed one pump system is the ease of engine anti-stall control. With the one eOC pump with complete controllability and pressure feedback, the engine anti-stall could be implement based on the engine available torque output at any given engine speed. The idea is to add the anti-stall controller right between the controller put of the supply pressure controller and the eOC pump controller as shown in Figure 9. First, the actual engine speed is feed into the engine map for the specific machine to obtain the maximum available engine torque that will not stall the engine. Then, a back calculation is performed to find the maximum allowable supply pump displacement that will not stall the engine using equation (10). When the available engine torque is higher than the maximum pump torque, the limited pump displacement $\beta_{P_{lim}}$ is greater than 1 and will not be used. The original pump displacement command goes through. But, when the system pressure increased to a certain level that might stall the engine, the controller will limit the pump command displacement to prevent engine stall.

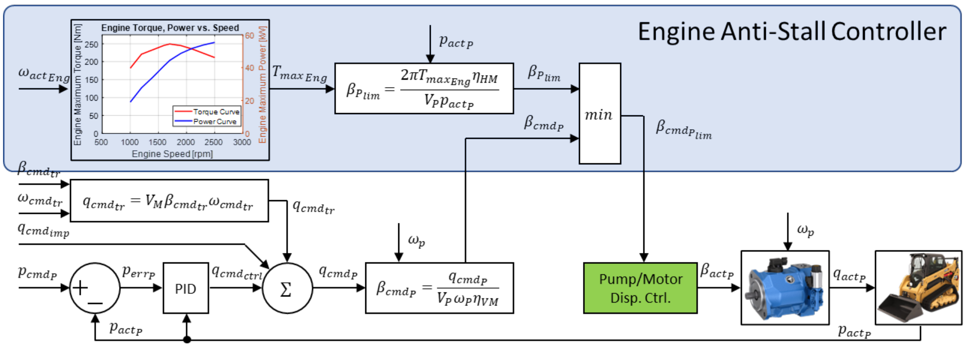

Figure 9. Engine Anti-Stall Controller.

$$\beta_{P_{lim}} = \frac{2\pi T_{max_{Eng}} \eta_{HM}}{V_P p_{act_P}} \tag{10}$$

3.5. *Flow Distribution Controller*

It is very likely that the total flow required by the drive system and implement exceed the maximum flow output of the pump. When that happens, the supply pressure will drop due to insufficient supply flow. Thus, the speed controller will command the motor to increase displacement to compromise for that pressure drop to keep the same torque output. This will lead to even worse flow deficit. This loop will happen very fast, and the pressure will crash and can never recover by its own. As a result, an anti-overflow controller must be added to prevent the system to go over the no-return point.

There are two rules defined in this controller. First, the implement holds the priority. Meaning when the total flow requirement exceeds the maximum supply flow, the drive system will automatically lower the motor displacement to free up more flow to ensure the implement can perform. In the meantime, the drive system required pressure will be recalculated with the limited motor displacement to compensate and keep same torque output. Second, when the limitation happens, the left and right track motor displacement limitation should hold same ratio $r_{L/R}$ to keep the flow balance between two tracks.

To achieve above rules, equation (11) - (15) are used to limit the motor displacement. The available flow for drive system $q_{dr_{lim}}$ is the lower one of the required flow $q_{cmd_{tr}}$ or what is left of the maximum pump flow subtract the implement system requirement $q_{cmd_{imp}}$. When flow saturation is happening, the motor beta command $\beta_{tr_{lim}}$ is scaled down with respect to the commanded speed ratio. In case of no limitation is needed, all terms will cancel out and leave $\beta_{tr_{lim}} = 1$, which means all 100% displacement is available.

$$r_L = \frac{\omega_{cmd_{tr_L}}}{\omega_{cmd_{tr_L}} + \omega_{cmd_{tr_R}}}, r_R = \frac{\omega_{cmd_{tr_R}}}{\omega_{cmd_{tr_L}} + \omega_{cmd_{tr_R}}} \tag{11}$$

$$q_{dr_{lim}} = min\left(\sum q_{cmd_{tr_{L/R}}}, q_{P_{max}} - q_{cmd_{imp}}\right) \tag{12}$$

$$q_{cmd_{tr_{L/R}}} = \omega_{cmd_{tr_{L/R}}} V_M \tag{13}$$

$$q_{P_{max}} = \omega_P V_P \tag{14}$$

$$\beta_{tr_{lim_L}} = \frac{q_{dr_{lim}} r_L}{V_M \omega_{cmd_{tr_L}}}, \beta_{tr_{lim_R}} = \frac{q_{dr_{lim}} r_R}{V_M \omega_{cmd_{tr_R}}} \tag{15}$$

4. Simulation and Results

4.1. Simulation Setup

A lumped parameter model is developed in Simulink environment as depicted in Figure 10. The model incorporates all controllers discussed in Section 3, along with the relevant components including the eOC units, engine, and vehicle. The models of these components are based on numerical expressions that account for efficiency losses and dynamic behaviours. While the focus of this study is on the controller design, the detailed modeling of each individual component is not covered in this section.

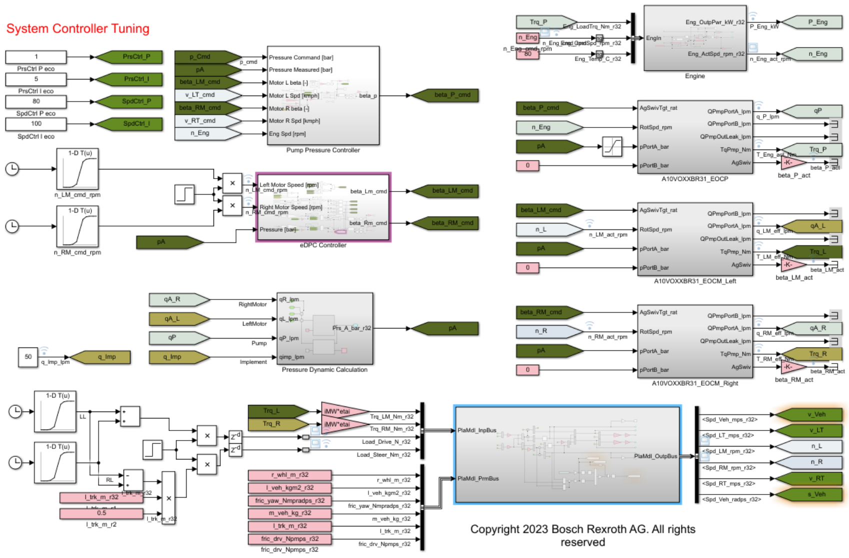

Figure 10. Simulation model developed in Simulink environment.

The inputs of the simulation are data from the baseline measurements on the reference vehicle. Figure 11 showcases a V-pattern drive cycle from the field. The first row shows the left and right motor load torque, and the second row shows the motor rotational speed.. For confidentiality of the baseline vehicle, the data are normalized according to the peak value. The torque is employed as the inputs to the kinematic model of the machine, and the motor speed is utilized as the user command. The target of the simulation is to investigate speed tracking performance with the complex loading conditions and compare the performance with the baseline regarding energy consumption and dynamic response.

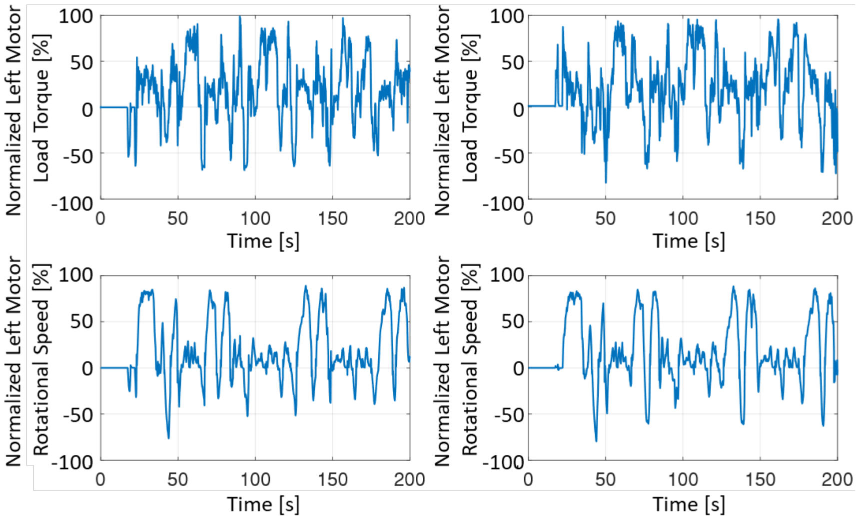

Figure 11. Baseline measurements of the track motor speed and torque.

4.2. *Steady State Simulation and System Efficiency Comparison*

Figure 12 depicts the system efficiency comparison between the proposed eOC-D system and the baseline machine. Focusing on the steady state performance, such as from 20s to 40s, the efficiency performance is fairly close and both are about 69%. However, this plot does not take power consumption of the charge pump into consideration. The eOC-D system does not require a charge circuit like the conventional closed-circuit. The reference machine employs a pilot pressure of 30bar with constant 55lpm flow, which results in about 2.8kW extra power consumption. If taking this value into account, the eOC-D system will have the overall efficiency advantage of 3% to 4%.

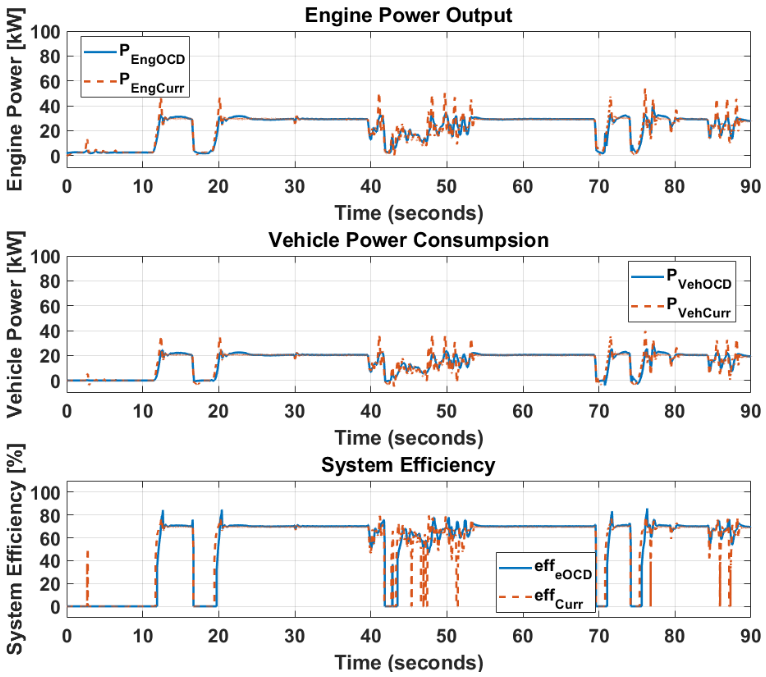

Figure 12. Steady-state simulation on the system efficiency comparison.

4.3. Dynamic Simulation and System Performance

4.3.1. No Implement Flowrate Performance

Figure 13 represents the simulation results based on the baseline measurements depicted in Figure 11. The three plots illustrate the pump displacement control, motor speed tracking, and system pressure, respectively. These results reflect the effective controller design detailed in Section 3 with proper parameters. In the second plot, the solid line is the command value and the dash line represents the simulated value. Overall, the motor speed tracking is good without apparent mismatch during all the transition phases.

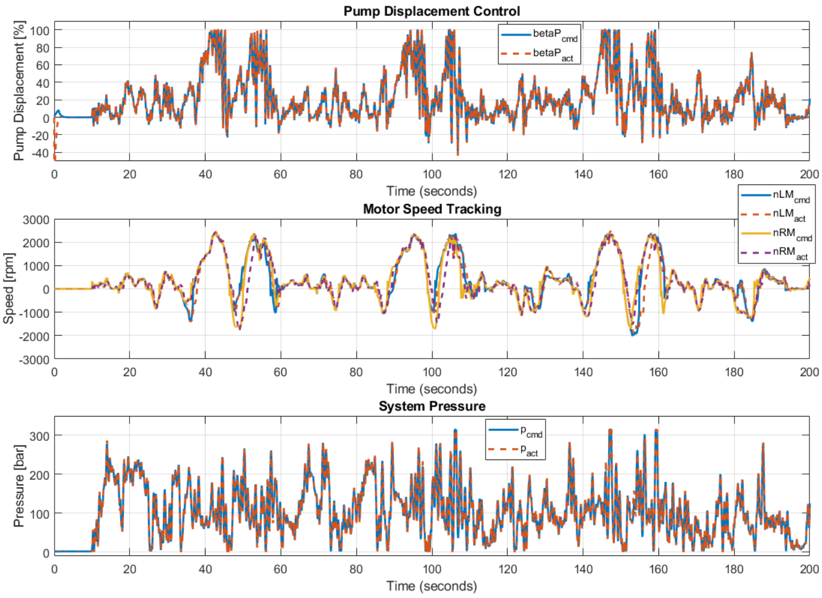

Figure 13. Simulation on dynamic performance, drive function only.

4.3.2. 50 lpm Implement Flowrate Performance

Figure 14 showcases another condition with drive and implement functions working at the same time. An extra 50lpm request is added to the pump with the same operation on the drive function. As explained in Section 3.5, the flow distribution controller gets activated. Compared to the results in Figure 13, the pump reaches the maximal pressure sometimes to meet the tractive torque demand with less motor displacement. With the proposed controller engaged, the speed tracking behaviour is still good and does not change obviously based on Figure 13.

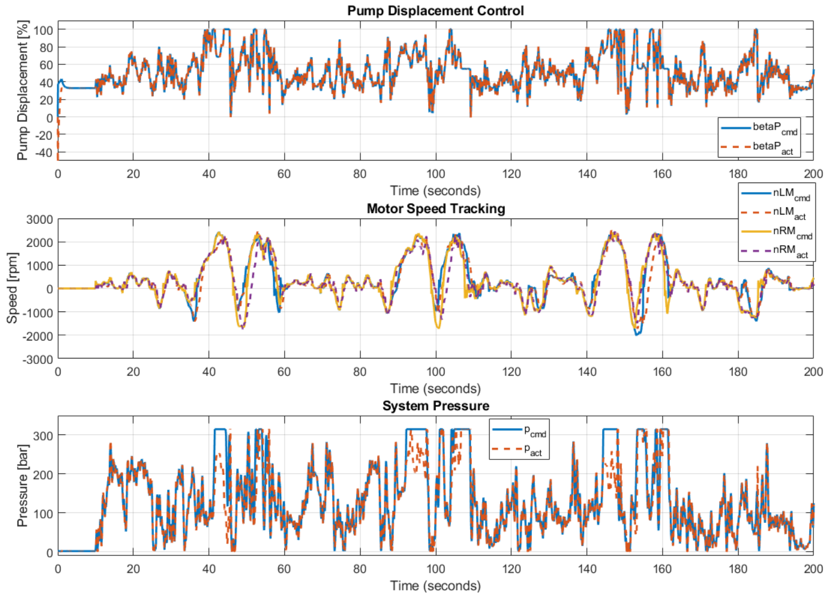

Figure 14. Simulation on dynamic performance, drive function and 50lpm implement requests.

5. CONCLUSION

This study proposed a novel eOC-D system aiming to improve the performance and reduce the component costs of the state-of-the-art hydrostatic transmission system. The development of the eOC-D architecture is based on a commercial compact loader. A comprehensive sizing study is conducted to determine the optimal combination of pump, motor and gearbox for the application, considering both the tractive torque and speed requirements. To overcome the control challenges of the new architecture, which uses only one pump for all functions, a detailed sequence of controller design is presented, from the component (eOC unit) level to the system level. The focus of this study lies in the controller, leveraging the capabilities of the eOC units to achieve the desired outcomes.

To evaluate the performance of the proposed architecture, a lumped-parameter model is built in Simulink environment. The simulation adapts the baseline measurements as inputs to reflect the realistic operating conditions. The simulation results indicate a comparable efficiency performance under steady-state scenarios. However, the simulation model does not include the charge circuit, which consumes extra power for the baseline system, thus giving a few percentage savings to the eOC-D architecture. On the other hand, the dynamic performance is remarkable due to the secondary control for the drive function.

At present, demonstration on the vehicle and more tests to validate the eOC-D design are undergoing. There are certainly some technical challenges to be addressed, especially for extreme loading conditions and simultaneously operation of the implement and traction. However, with the advantages of component costs reduction, the proposed architecture could be a popular solution to replace the traditional hydrostatic transmission system.

6. References

[1] X. Guo and A. Vacca, “Advanced Design and Optimal Sizing of Hydrostatic Transmission Systems,” *actuators,* vol. 10, no. 9, p. 243, 2021.

[2] N. Nervegna and M. Rundo, Passi nell'oleodinamica. Vol. 1-2., 2020.

[3] G. L. Zarotti, “Trasmissioni idrostatiche.,” *Istituto per le Macchine Agricole e Movimento Terra,* pp. 707-2003, 2003.

[4] A. Vacca and G. Franzoni, Hydraulic Fluid Power: Fundamentals, Applications, and Circuit Design, Wiley, 2021.

[5] G. Costa and N. Sepehri, Hydrostatic Transmission and Actuators: Operation, Modelling and Applications, Hoboken, NJ, USA: John Wiley & Sons, 2015.

[6] N. Keller and M. Ivantysynova, “A New Approach to Sizing Low Pressure Systems,” in *ASME/BATH Symposium on Fluid Power and Motion Control*, 2017.

[7] S. Tetik and M. Brand, “Secondary Control Based Hydraulic Architectures For Mobile Applications,” in *The 13th International Fluid Power Conference*, Aachen, Germany, March 21-23, 2022.